Exploration of plant-based leaf extracts as anti-corrosive concrete admixtures for extending the service life of reinforcement concrete infrastructures

Jivan Raj Dhungana[1], *Madhab* Gautam[1,2], *Dhruba Babu* Subedi[1], *Nootan Prasad* Bhattarai[1*], and *Jagadeesh* Bhattarai [1†]

[1]Central Department of Chemistry, Tribhuvan University, Kirtipur 44618, Kathmandu, Nepal.
[2]Department of Chemistry, Tribhuvan M. Campus, Tribhuvan University, Tansen 32500, Palpa, Nepal.

Abstract. This study intended to improve the service life of reinforcing mild steel (MS) within concrete beams (CBs) by incorporating leaf extracts from *Justicia adhatoda* L. (JAL) and *Persea americana* Mill. (PAL) as concrete admixtures in corrosive environmental conditions. The research involved monitoring the corrosion susceptibility levels of mild steel-reinforced concrete beams (MS-CBs) with varying concentrations of JAL and PAL extracts—specifically, 500, 1000, 2000, and 4000 ppm. Half-cell potential (HCP) and electrical resistivity (ER) data were collected for seven months or more, following ASTM standards, and were recorded at various time intervals to ensure accurate assessment. The outcomes indicated that the corrosion resistance of the MS in CBs significantly improved with 500-4000 ppm of these extracts as a concrete admixture, as compared with the corrosion level of the MS-CBs without extract (control). Phyto-screening analysis has identified key bioactive components, including alkaloids, flavonoids, and tannins. FTIR and UV-visible analysis results validate the conclusions drawn from the phyto-screening tests. Scanning electron microscopy (SEM) analysis provides pertinent surface information regarding the MS in CBs, yielding valuable insights into the chemical composition that may facilitate the development of novel anti-corrosive films for corroded MS, thereby mitigating early corrosion damage in MS-CBs and elucidating the corrosion inhibition mechanism. The study highlights the potential of plant-based inhibitors to enhance the durability of reinforced concrete, offering practical benefits for infrastructure longevity and guiding future research in sustainable construction materials.

1 Introduction

Concrete is one of the most widely used structural materials in modern engineering due to its excellent compressive strength; however, it exhibits relatively low tensile strength [1]. To address this limitation, reinforcement using steel rebar has become standard practice, leading to the development of reinforced concrete [2]. In its initial state, concrete has a high pH (above 12), which promotes the formation of a passive oxide layer on the reinforced metal surface, protecting it from corrosion [3]. However, the ingress of aggressive environmental pollutants through the concrete's pores can lower the pH below 10, dissolve or break down the passive layer, and hence initiate corrosion [4]. The results ultimately lost the structural integrity of the reinforcement concrete infrastructures [5].

Corrosion of reinforcement concrete is a progressive and unavoidable process. The interaction between environmental contaminants and MS surfaces, facilitated by the porous nature of concrete, is a key factor in MS-CBs corrosion [6]. It can mitigate but cannot be avoided completely. Many mitigation strategies include the use of coated rebars [7] and corrosion-inhibiting admixtures [8]. However, the coated reinforcement rebars did not provide total protection in reinforced concrete (RC). Their use does not effectively reduce the damage caused by chloride-induced corrosion when compared with uncoated bars embedded in concrete with similar characteristics [9].

Besides the use of coated rebars to control the early corrosion damage of MS in RC structures, synthetic organic and inorganic waterproofing chemicals effectively inhibit corrosion in reinforced concrete structures where safety is critical [10]. These waterproofing chemicals are commonly used in both commercial and residential projects to create impermeable concrete by reducing its porosity [11] and filling its pores and capillaries [12]. The ingress rate (Ri) of moisture or pollutants through concrete capillaries is proportional to the fourth power of the capillary radius (r), noted as $Ri \propto r^4$ [13]. It means even minor alterations in pore size can affect the rates at which corrosion-

* Corresponding author : neutan08@gmail.com
† Corresponding author : bhattarai_05@yahoo.com

enhancing moisture penetrates and influence the permeability of pollutant gases.

The usage of cement-based WProf additives can help to reduce capillary diameter and slow down the degradation of concrete structures [14]. It is achieved through the formation of hydrated calcium silicate (C-S-H) gel when using waterproofing chemicals as concrete additives [15]. However, such waterproofing chemicals have exhibited toxic, carcinogenic, and environmentally harmful properties. Therefore, in recent decades, cost-effective and eco-friendly plant-based inhibitors have been crucial in mitigating the corrosion of metals and their alloys. Consequently, this work has prompted us to seek greener concrete admixtures.

There has been increasing interest in developing green corrosion inhibitors derived from components of natural plants found in Nepal to mitigate the corrosion of metals and their alloys including the mild steel. As a result, in response to the necessity for eco-friendly alternatives to synthetic waterproofing agents and the corrosion-prone inorganic and organic compounds affecting RC infrastructure, recent research has focused on the potential of green corrosion inhibitors derived from plant sources as concrete admixtures.

Nepal's flora offers significant opportunities to identify natural inhibitors that control concrete corrosion, integrating them into concrete formulations to enhance the durability of RC structures. In this context, a primary objective of this investigation is to develop an environmentally sustainable anti-corrosive concrete admixture derived from the leaves of two Nepali plants, *Justicia adhatoda* L. (JAL) and *Persea americana* Mill. (PAL), named as Asuroo (Malabar nut) and Avocado, respectively, in Nepali.

Both plant-based extracts are promising green alternatives for corrosion inhibition due to the formation of protective adsorption layers—either physically or chemically—on the surface of mild steel through interactions between their bioactive components and iron atoms. Avocado (*Persea americana* Mill.) has gained popularity because of its rich nutritional profile and potential health benefits [16]. Research has identified a wide range of secondary phytochemicals in avocado extracts, including carotenoids, flavonoids, alkaloids, terpenoids, and long-chain fatty alcohols [17]. Studies have also explored the use of avocado seed extract as an eco-friendly corrosion inhibitor for mild steel in 0.5 M sulfuric acid, employing both gravimetric and electrochemical methods [18]. Another study found that avocado leaf extract effectively acts as a green corrosion inhibitor in acidic solutions [19].

Similarly, *Justicia adhatoda* L., commonly known as Malabar nut in English, is a plant belonging to the Acanthaceae family. It contains various bioactive phytoconstituents, including alkaloids, phytosterols, polyphenols, and glycosides [20]. The effectiveness of the leaf extract from this plant as a corrosion inhibitor was evaluated on mild steel in aqueous neutral electrolyte using weight loss, corrosion potential, and potentiodynamic polarization methods [21].

To the best of the authors' knowledge, this study is the first to explore the use of *Justicia adhatoda* L. (JAL) and *Persea americana* Mill. (PAL) leaf extracts as corrosion-inhibiting concrete admixtures. The researchers investigate the anti-corrosive performance of these extracts under ambient conditions using the HCP and ER methods in compliance with ASTM standards [22]. Complementary surface analyses further support the findings. This work contributes to the development of eco-friendly, cost-effective, and sustainable corrosion inhibitors or concrete admixtures for use in reinforced concrete structures.

2 Materials and methods

Mature and healthy leaves of the *Persea americana* (Mill.) and *Justicia adhatoda* (L.) plants were collected from Tanglaphant in Kirtipur Municipality, Kathmandu, and Janaki Rural Municipality in the Durgauli area of Kailali district, respectively. The leaves were cleaned individually several times using distilled water and then air-dried, placing them in shaded areas for 25 days. An electric mill was used to grind the dried leaves of each plant into a fine powder for preparing individual plant extracts.

Roughly 400 g of pulverized leaf powder of each plant was weighed and mixed separately into seven 2000 mL conical flasks containing 800 mL of methanol. After being tightly sealed and thoroughly shaken, they were kept for 2 weeks or more with regular shaking. The mixtures were filtered using Whatman filter paper. Excess methanol in the filtrate was concentrated using a rotary evaporator (IKA RV 10 digital V, Germany) (as illustrated in Figure 1) to remove residual methanol from each extract, yielding semi-solid forms of the leaf extracts from *Persea americana* (PAL) and *Justicia adhatoda* (JAL), as described elsewhere [24].

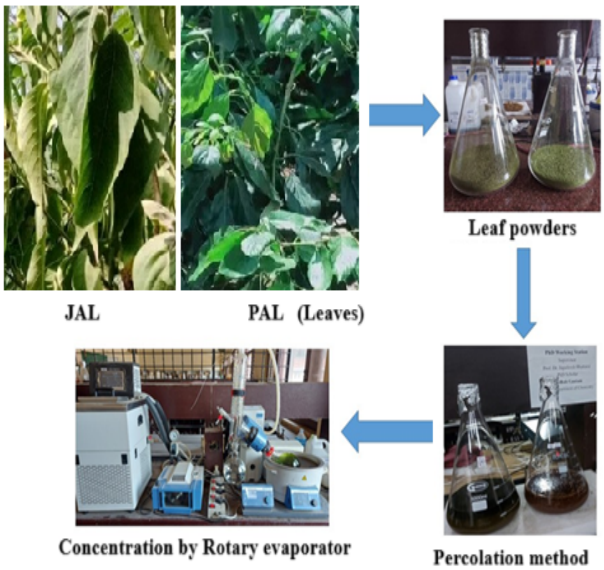

Fig. 1. Steps for JAL and PAL preparation.

These extracts were subsequently transferred to a container to evaporate the remaining methanol, which acts as a concrete admixture or as an eco-friendly corrosion inhibitor. Both semi-solid extracts were stored separately in a freezer at 4°C or lower before being mixed with concrete aggregates.

A mold box measuring 36 cm × 9 cm × 9 cm was used for preparing the MS-CBs [Figure 2(d)]. Initially, sets of concrete mixtures were prepared using a ratio of 1:2:3 for cement, sand, and gravel [Figure 2(a)], with a water-to-cement ratio of 0.45 per ASTM C1582/C1582M-11 standard [22]. The required amounts of the plant extract dissolved in distilled water for preparing the concrete paste [Figure 2(c)]. The concrete paste, with or without the addition of plant extracts, was poured into the molds, embedding a 10 mm diameter mild steel rebar into each beam. The beams without any extracts served as the control MS-CB.

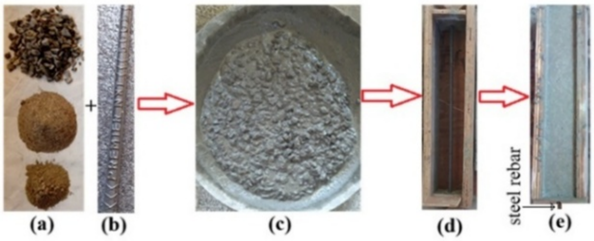

Fig. 2. Materials of MS-CB preparation [cement-sand-gravel (a), mechanically and chemically cleaned MS rod (b), concrete paste (c), MS rod fix in a casting box (d), and MS-CB (e)].

Before embedding, each mild steel rebar (MSR) was cleaned with silicon carbide sandpaper, treated in concentrated HCl and Na_2CO_3 solution, and then washed with distilled water. To record the half-cell potential (HCP), as demonstrated in previous research by Roka et al., 2 cm of the MS rebar was intentionally left exposed at one end of the MS-CB. The exposed end of the MS rebar (i.e., the 2 cm MS rebar left outside the reinforced concrete beam) functions as a working electrode to which the positive pole of the digital multimeter is connected, as demonstrated in Figure 2(e) as well as in Figure 3.

A total of eight sets of steel-reinforced concrete beams were produced using varying concentrations of JAL and PAL, ranging from 500 to 4000 parts per million (ppm) [Figures 3(a) and 3(b)]. Each MS-CB surface has marked four points just above the embedded MS to record the in-situ electrochemical properties of HCP and ER. The average of these four points of each MS-CB was calculated with standard error values (n=4).

After casting, all beams were cured at room temperature (25 ± 2°C) for one week. Following this period, the HCP and ER were recorded periodically over seven months. A digital multi-meter was employed for these measurements, utilizing a saturated calomel electrode (SCE) as the reference electrode (RE) and the exposed MS rebar as the working electrode (WE). For consistent measurement of HCP and ER, four equally spaced points labeled 1 through 4 were marked on the top of each MS-CB, as illustrated in Figures 3 (a) and 3(b).

The HCP and ER values were determined by connecting the negative terminal of the multi-meter to the reference SCE electrode and the positive terminal of the multi-meter to the exposed end of the MS rebar. To measure the HCP and ER, the SCE electrode was inserted in a moistened sponge and positioned directly above every four points of MS-CBs. The corrosion level can be inferred from the measured average values of HCP and ER, as outlined in Table 1 [24].

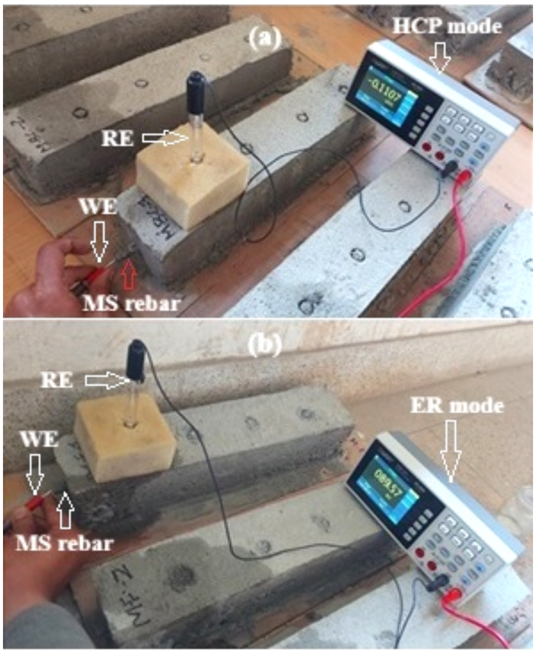

Fig. 3. Experimental set up for measurement of HCP (a) and ER (b).

Table 1. Correlation between HCP and ER values with corrosion risk level of MS-CBs [31].

HCP (mV vs SCE)	**ER (kΩ.cm)**	**Corrosion risk level of MS-CBs**
< -276	<10	High or more than 90 % corrosion risk (HiC)
−276 to −126	10 to 20	Mild or 10-90% of corrosion risk (MiC)
> −126	> 20	Low or less than 10 % of corrosion risk (LoC)

The JAL and PAL, utilized as concrete admixtures, were characterized using UV-Vis (SPECORD®200PLUS, Germany), FTIR (IR Affinity-1S, SCHIMADZU), GC-MS (Agilent 7890B Gas Chromatograph coupled with a 5977A Mass Selective Detector), and ultra-high-performance liquid chromatography (UHPLC) (XEVO G2-XS QTOF, Waters Corporation, USA) analysis to analyze the electronic properties of secondary metabolites (SeMBs), their functional groups, identify the number and confirm the presence of varieties of SeMBs in both plant extract. The surfaces of MS before and after reinforcement in CBs were analyzed using optical and scanning electron microscopic (Tabletop SEM-TM 4000, Hitachi).

The JAL and PAL, utilized as concrete admixtures, were characterized using UV-Vis (SPECORD®200PLUS, Germany), FTIR (IR Affinity-1S, SCHIMADZU), GC-MS (Agilent 7890B Gas Chromatograph coupled with a 5977A Mass Selective Detector), and ultra-high-performance liquid chromatography (UHPLC) (XEVO G2-XS QTOF, Waters Corporation, USA) analysis to analyze the electronic properties of secondary metabolites (SeMBs), their functional groups, identify the number and confirm the presence of varieties of SeMBs in both plant extract. The surfaces of MS rebar before and after reinforcement in CBs were analyzed using optical and scanning electron microscopic (Tabletop SEM-TM 4000, Hitachi).

3 Results and discussion

Based on the phytochemical screening test [21], the methanolic leaf extracts of *Justicia adhatoda* (JAL) and *Persea americana* (PAL) show positive tests for phenols, alkaloids, flavonoids, and terpenoids. In contrast, both plant extracts show negative tests for saponins and steroids (as shown in Table 2).

These phyto-compounds have shown prospective action, developing a corrosion-resistant passive film on the surface of MS rebar in CBs. The findings of the phyto-compound screening tests conducted in this study are consistent with previously reported data on the methanol extract prepared from the leaves of *Justicia adhatoda* [25] and *Persea americana* [26].

Table 2. Screening tests for constituents present in JAL and PAL.

Constituent	Test name/agent	JAL	PAL
Phenols	Lead acetate	+	+
Alkaloids	Dragendroff's test	+	+
Saponins	Foam	−	−
Flavonoids	Alkaline	+	+
Glycosides	Legal	−	+
Tannins	Ferric chloride	+	−
Terpenoids	Salkowski	+	+
Carbohydrates	Molisch Reagent	−	+

('+' refers to the presence and '-' refers to the absence)

The UV-Vis peaks of JAL and PAL were recorded between 200-800 nm wavelength due to the presence of secondary metabolites [27], as illustrated in Figures. 4(a) and 4(b), respectively. The JAL and PAL exhibited distinctive peaks at the range of 250-700 nm wavelength or ultraviolet/visible region and for the π-conjugation of single-double bonds in secondary metabolites or chlorophyll when subjected to UV-visible spectroscopy, which revealed the presence of alkaloids, flavonoids, terpenoids, and phenols, as reported in the literature [28]. Doublet peaks at 268 nm and 273 nm for JAL are due to the presence of -OH, $-OCH_3$, -CN, or -COOH groups attached to aromatic ring compounds [29], which are difficult to observe for PAL. Literature has noticed that the UV-Vis peak around 270-280 nm represents the presence of phenolic groups in guava leaf extract [30]. Furthermore, the UV-Vis bands at 288 nm and 332 nm demonstrated the existence of tannins and phenolic compounds, respectively, as in the literature [31].

Similarly, peaks observed around 330 nm and 380 nm are due to the presence of flavonoids in PAL and are difficult to observe for JAL. A peak at 405 nm is due to the presence of terpenoids, as reported elsewhere [29]. The peak around 663-665 nm is due to the presence of chlorophyll. The peak observed around 320-332 nm is due to the presence of flavonoids in the plant extracts. In the same way, any peaks that are not around 210-220 nm indicate the absence of saponins in both JAL and PAL extracts [32]. The depicted phyto-compounds contain σ-bonds, π-bonds, lone pairs of electrons, chromophores, and aromatic ring compounds, per existing literature [33].

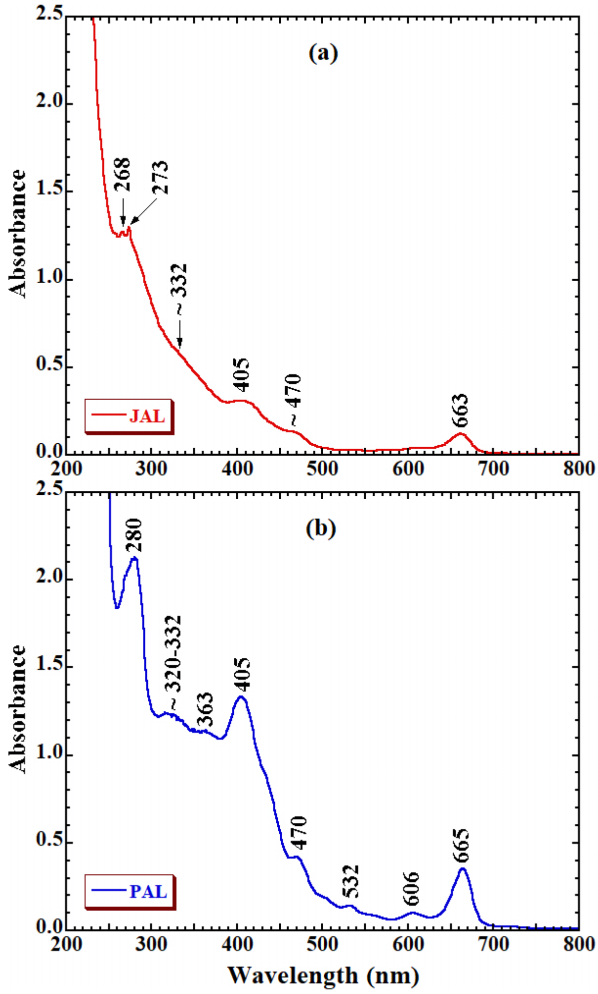

Fig. 4. UV-Vis Spectra analysis of JAL (a) and PAL (b).

FTIR analysis allows for the identification of functional groups present in plant extracts. Figures 5(a) and 5(b) display the FTIR spectra recorded for the JAL and PAL, respectively. The symmetric and broad absorption peak around 3340-3230 cm^{-1} corresponds to the O-H stretching of hydroxyl compounds [34]. These functional groups are characterized by specific peaks, at around 3200-3400 cm^{-1} for O–H stretching vibration in aromatic compounds [35], 1606-1617 cm^{-1} for aromatic C = C stretching [36], 1446 cm^{-1} for C–H stretching [37], 1201 cm^{-1} for –COOH group [38], 1038 cm^{-1} for O–H or C–H bending of aromatics [39], suggesting the presence of phenolic or alcoholic compounds [40]. Besides, Peaks around 2927 cm^{-1} represent asymmetric C-H stretching vibrations of both the JAL and PAL. These results are consistent with previous studies on the same plant extracts [41]. The presence of secondary or tertiary amino in the JAL is confirmed by two peaks around the 1100-1200 cm^{-1} range, indicating the C-N stretching vibration [42].

GC-MS analysis revealed the presence of 25 and 28 secondary metabolites (SecMs) in JAL and PAL extracts respectively, as demonstrated in Figure 6. It is meaningful to mention that the methanol leaf extract of this plant yielded only 13 phyto-compounds from GC-MS analysis [43]. GC-MS analysis data are imported into MZmine software in the form of mzML files to encourage the matching of m/z values and retention times with reference database libraries. This procedure is critical for the identification and quantification of compounds within complex samples.

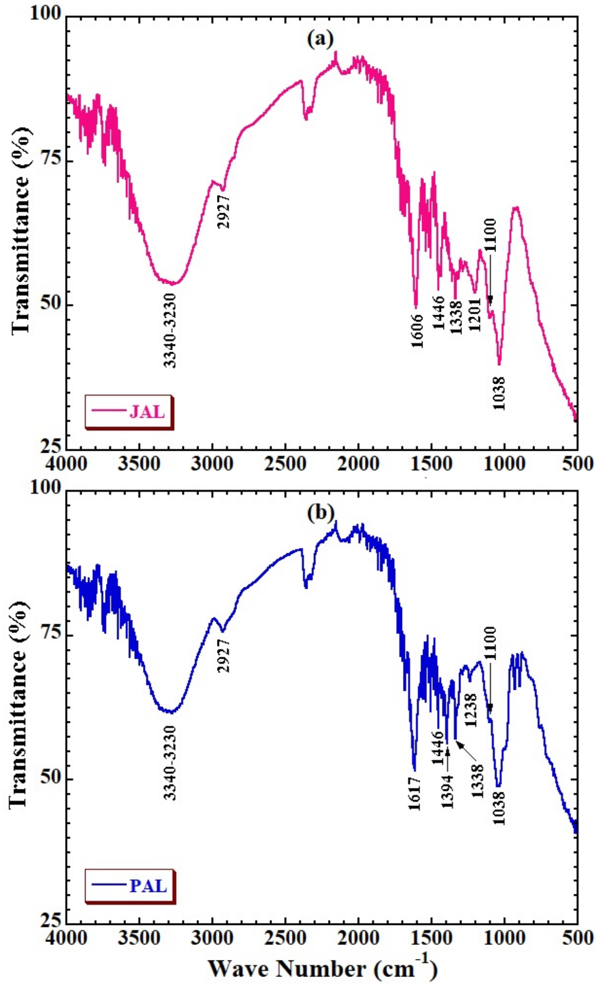

Fig. 5. FTIR Spectra analysis of JAL (a) and PAL (b).

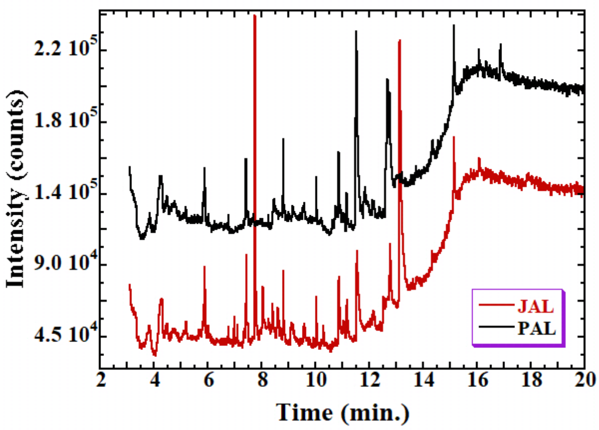

Fig. 6. GC spectra of JAL and PAL for qualitative phyto-compounds analysis.

It suggested that the presence of β-caryophyllene, 3-methylene-7, 11-dimethyl-1-dodecene, nonadecanoic acid methyl ester; 9, 12-octadecadienoic acid (Z, Z)-methyl ester, and 2-napthalene sulfonic acid are the main phyto-compounds in JAL extract, while DL-2-hydroxybutyric acid, penta-ethylene glycol dimethyl ether, 3-methylene-7, 11-dimethyl-1-dodecene, nonadecanoic acid methyl ester, 5-phenyl-3, 5, 7-triaza-tetracyclo, 2-napthalene sulfonic acid, *etc.* are in PAL extract. These qualitative consequences exhibited that both JAL and PAL have powerful anti-corrosive effects, contributing to the corrosion prevention of MS-CBs.

An ultra-high performance liquid chromatography (UHPLC) method, which is assumed to be more reliable than UV-Vis, FTIR, and GC-MS methods, was employed to detect the presence of various SeMBs in the methanolic extracts of JAL and PAL. Although the complete analysis and identification of all compounds by UHPLC analysis can be challenging when using crude extracts instead of isolated compounds [44], the most abundant compounds are expected in PAL and JAL, as summarized in Tables 3 and 4, respectively. Alkaloids, flavonoids, terpenoids, and phenolic compounds were in both extracts through the MassBank search page (https://massbank.eu/MassBank/Search), which provides access to a comprehensive database of mass spectral data.

Table 3. Major presumed phyto-compounds present in JAL.

Ret. Time (min.)	Molecular Formula and Molecular Weight (g/mol)	Phyto-compounds	Classification
4.94	$C_{15}H_{20}O_4$ (264)	Abiscisic acid	Terpenoid
6.77	$C_{40}H_{56}$ (537)	Beta-carotene	Terpenoid
14.26	$C_{21}H_{14}O_7$ (378)	Justicidin G	Lignan/Phenol
15.19	$C_{20}H_{24}N_2O_2$ (324)	Quinine	Alkaloid
15.36	$C_{25}H_{20}O_{10}$ (482.4)	Silychrystin	Flavonoid

Table 4. Major presumed phyto-compounds present in PAL.

Ret. Time (min.)	Molecular Formula & Molecular Weight (g/mol)	Phyto-compounds	Classification
5.26	$C_{15}H_{14}O_6$ (290.3)	Epicatechin	Flavonoid
7.70	$C_{21}H_{20}O_{11}$ (448.4)	Maritimein	Flavonoid
14.71	$C_{21}H_{24}O_6$ (372.4)	Arctigenin	Polyphenol
18.28	$C_{25}H_{22}O_{10}$ (482.4)	Silychristin	Flavonoid
18.83	$C_{33}H_{49}NO_8$ (587.7)	Pseudojervine	Alkaloid
20.03	$C_{25}H_{22}O_{10}$ (482.4)	Silybin B	Flavonoid

The presence of these alkaloids, flavonoids, terpenoids, and phenolic phyto-compounds, which are characterized by aromatic rings, heteroatoms, and conjugated systems, as indicated by UV-Vis, FTIR, and phytochemical profiling tests also. These secondary metabolites in JAL and PAL extracts are supposed to be the basis of the results of UHPLC analysis using mass bank matching. These metabolites included flavonoids, alkaloids, terpenoids, pyridine, and phenolic compounds, as illustrated by their molecular formula in Figures 7 and 8.

These aromatic rings, heteroatoms, and conjugated systems present in phyto-compounds improve both physical and chemical adsorption processes, as proposed in the literature [45]. This interaction helps to form a diffusion-barrier passive film between the corroded MS rebar and the concrete mix. These findings underline the perspective of JAL and PAL as anti-corrosive agents for preventing the corrosion of MS-CBs. Moreover, the secondary metabolites (SecMBs) found in both plant extracts offer insights into the adsorption mechanisms that create a protective passive film on the surfaces of corroded MS in CBs, as discussed in a succeeding section.

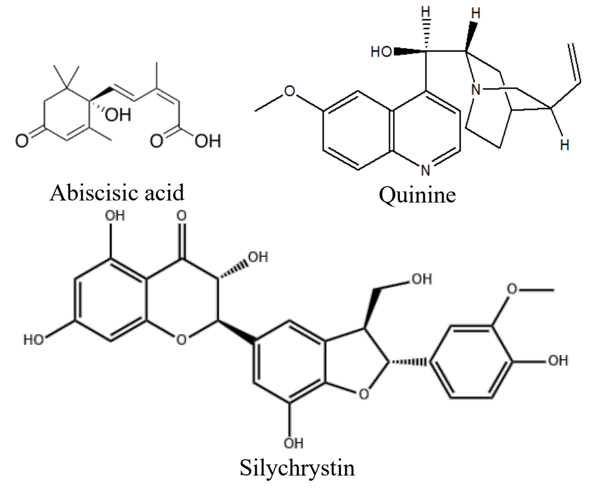

Fig. 7. Molecular structure of some phyto-compounds assumed to be present in JAL from UHPLC analysis.

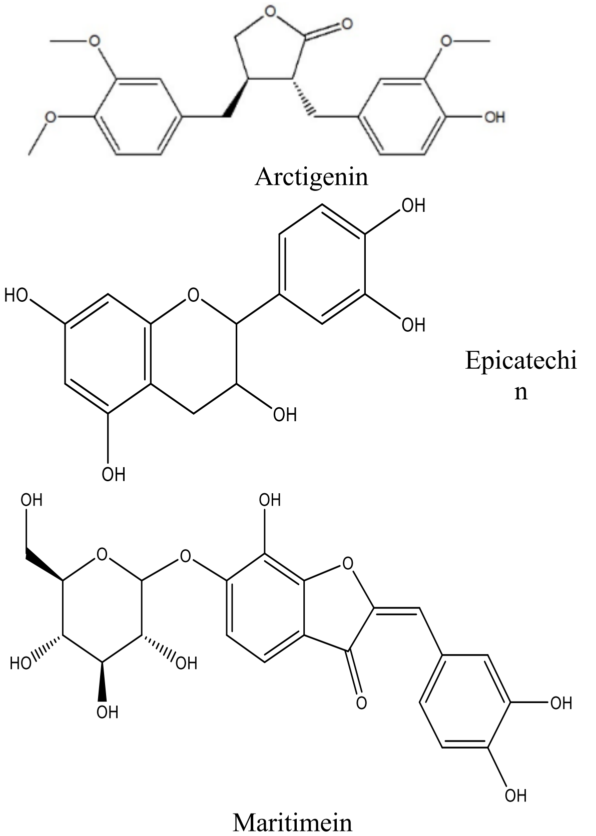

Fig. 8. Molecular structure of some phyto-compounds assumed to be present in PAL from UHPLC analysis.

The half-cell potential (HCP) values were measured at four different points on the surface of the MS-CB for 220 days to investigate the effect of 500-4000 ppm JAL and PAL. The trend of HCP changes of all four types of MS-CBs with 500 ppm, 1000 ppm, 2000 ppm, and 4000 ppm JAL and PAL are almost the same except in the case of control-MS in CB without extract, as illustrated in Figures 9(a) and 9(b), respectively. These findings suggest a positive impact of JAL and PAL on the corrosion-resistant properties of MS in CBs.

The results of the HCP measurements indicate that the potential value of the control-MSReC shifted to more negative values (i.e., at the MiC zone) with exposure times after 31 days, as illustrated in Figure 9. However, at the initial exposure time between 7 and 31 days, the CorP of the control-MS in CB shifted to less negative potential regions than -126 mV (SCE) with exposure times until about two months, suggesting the corrosion risk remains in LoC regions (with less than a 10% probability of corrosion risk) even the control-MS in CB according to the ASTM C876-22b standard [24].

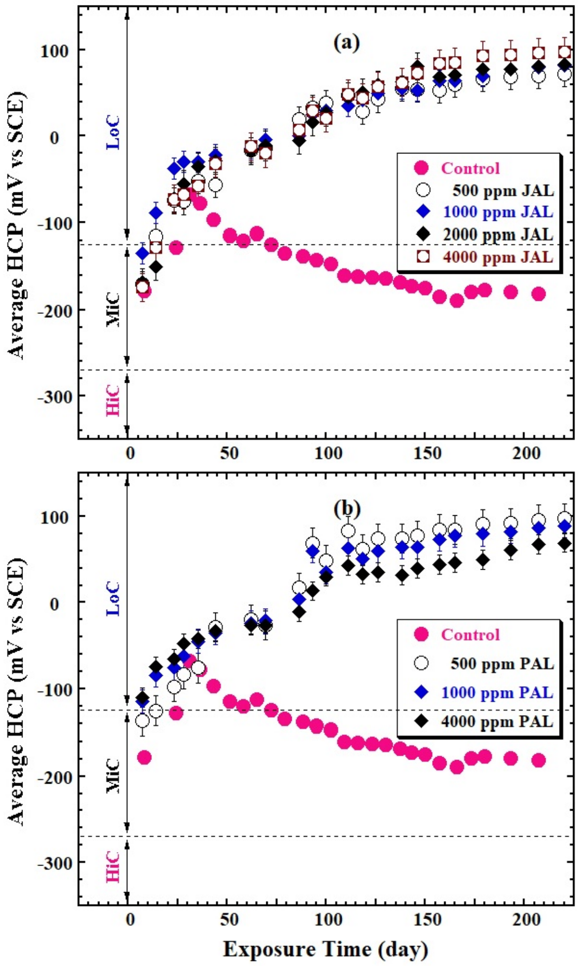

Fig. 9. Variation of average HCP of ReMS in ReC beams without and with 500-4000 ppm of (a) JAL and (b) PAL in ambient environment, as a function of exposure time.

In contrast, the concrete beams treated with 500-4000 ppm plant extracts showed HCP values in the MiC regions at the initial 3 to 4 weeks of exposure. These values likely indicate a preliminary stage of a protective thin film formation on the MS rebar in CBs with various concentrations of the plant extract. As a result, the probability of reinforced concrete corrosion located between 10% and 90% (MiC), with HCP values ranging from -276 mV to -126 mV (SCE). This phenomenon occurs during the early stages of the corrosion process, triggered by the penetration of moisture, oxygen, CO_2, and other harmful atmospheric agents into the MS-CBs.

Therefore, it is crucial to address this issue promptly to prevent further deterioration and ensure the long-term durability of the reinforced concrete structures. The HCP values shifted towards a more noble region or greater than -126 mV (SCE), indicating a low corrosion risk with less than 10% corrosion probability (LoC). This shift of HCP from MiC to LoC region, attributing to the formation of a protective thin film over the MS rebar in concrete mix with different concentrations of JAL or PAL, as shown in Figures 9(a) and 9(b). The formation of such thin and diffusion barrier film protects the concrete beams efficiently from corrosion with the addition of JAL and PAL extract as concrete admixtures.

The determination of electrical resistivity (ER) values, based on the results obtained from HCP data, becomes a valuable supportive tool for assigning three corrosion levels of the MS-CBs corrosion, as per the ASTM C876-22b standard [21]. The recoded ER-values for the control MS-CB without plant extract over 220 days decreased during the measurement period due to the penetration of aggressive or corrosive ions of molecules like Cl^-, SO^{2-}_4, H_2O, and O_2 through the pollutant atmosphere, and thus are responsible for the higher conductivity in the embedded MS surface as there was no formation of thin film in the absence of plant extract. Therefore, in turn, this resulted in increased conductivity on the surface of the embedded MS, as illustrated in Figure 10.

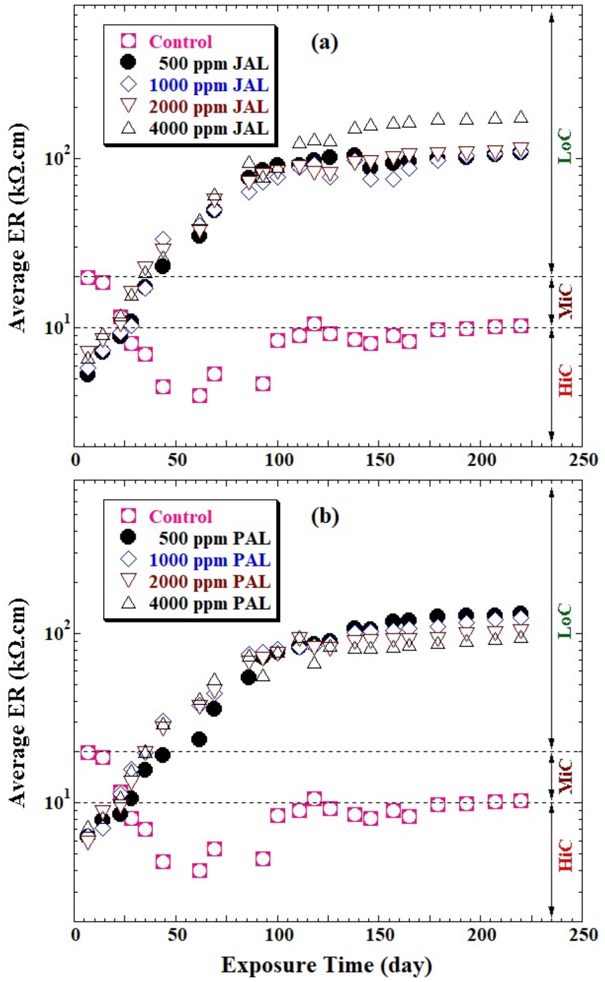

Fig. 10. Variation of average electrical resistivity (ER) of reinforcing MS in different CBs without and with 500-4000 ppm of (a) JALE & (b) PALE in ambient environment, as a function of exposure time.

The lack of a thin film formation on the surface of MS rebar in the absence of plant extract facilitated the ease with which the pollutant gases, molecules, or ions could penetrate the concrete surface. Conversely, the other eight CBs, each reinforced with different concentrations of individual plant extracts (500-4000 ppm of JAL or PAL), demonstrated a consistent increase in resistivity value up to 220 days, as shown in Figure 10, attributing to the reduced possibility of aggressive ions ingress to the embedded MS rebar surface. It is noteworthy that these findings have practical significance since they can enhance the durability and longevity of reinforced concrete structures.

Moreover, these results of the present work are compatible with the previous study, which reported the efficacy of the leaf extracts of *Ziziphus budhensis* and *Tagetes erecta* L. [22] and *Sesamum indicum* L. [46], as eco-friendly corrosion inhibitors in a saturated $Ca(OH)_2$ solution with a pH 12 ± 0.5, considered as SCPS (simulated concrete pore solution), and mango fruit extract in SCPS [54], which mimics the environment of CB. The weight loss and electrochemical polarization assessed the ability of these plant-based extracts to inhibit steel corrosion, and the highest corrosion-inhibition efficiency was reported to be 80%-95%. These extracts contain secondary phyto-molecules that adhere to the metal surface in SCPS.

An analysis of the MS-CBs containing varying amounts of JAL and PAL extracts indicates a low corrosion risk of MS rebar in CB. This outcome was attributed to the formation of a protective thin film over the surface of the embedded rebar. Consistent with this finding, HCP measurements also indicated a reduced likelihood of corrosion. These observations suggest that the use of plant extract in MS-CBs could be a promising approach to mitigating reinforcement corrosion in concrete structures.

Further investigation of the morphological changes on the MS rebar surface after being embedded for seven months in the concrete beams, without (control) and with 2000 ppm JAL or PAL, was explored using SEM analysis. The SEM images of the MS surface in the control MS-CB without plant extract show patches of rust and pits over large areas of the sample, as illustrated in Figure 11. This surface of MS rebar indicates the corrosion of the rebar embedded in the control beam.

However, surface flaws related to rust are not visible in the SEM images of the MS in CB when mixed with 2000 ppm of JAL or PAL inhibitors, as shown in Figures 12(a) and 12(b), respectively. Smooth and uninterrupted corrosion-protective layers form on the MS surface by eliminating active corrosion sites through the adsorption mechanisms of the phyto-molecules present in these plant extracts, as outlined in previous studies [45].

The SEM images indicate that corrosion-related surface imperfections have been removed or minimized on the inhibited surface, highlighting the increased effectiveness of the two plant extracts in providing corrosion protection. As a result, incorporating 2000 ppm of JAL and PAL extract into the concrete mix reduces the likelihood of SR corrosion damage from the microbiologically influenced corrosion (MiC) zone to a passive state (i.e., LoC). According to the literature [48], the phyto-molecules of the plant extract acts as efficacious adsorbents, promoting the reduction of active corrosion sites on the surface of MS rebar.

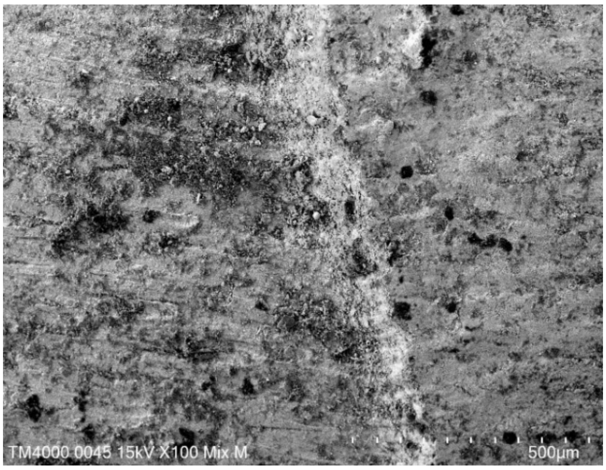

Fig. 11: SEM images of the MS rebar surface after embedded for 7 months in control CB without extract.

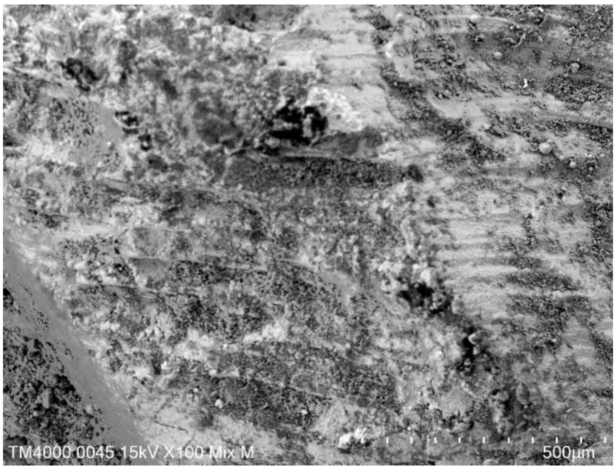

(a) 2000 ppm JAL

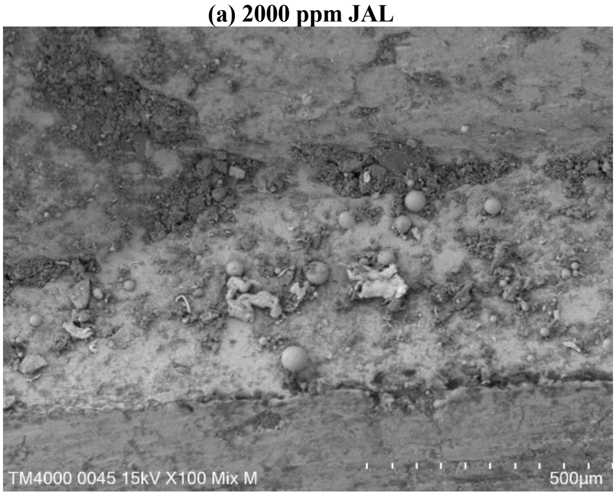

(b) 2000 ppm PAL

Fig. 12. SEM images of the MS rebar surface after embedded for seven months in CBs with 2000 ppm of (a) JAL, and (b) PAL.

The SEM images of the MS embedded in CB with phyto-compounds furnish compelling evidence that surface flaws associated with corrosion have been successfully eliminated on the inhibited surface, thereby demonstrating the improved inhibition effectiveness of the JAL and PAL in MS-CB corrosion. Consequently, the probability of MS corrosion damage has shifted from MiC to LoC region with the addition of 500-4000 ppm JAL/PAL into the MS-CBs.

The findings from the SEM analysis align with the results related to HCP and ER measurement methods, as discussed previously. A superior inhibition potential of these two plant-based extracts furnishes evidence to sustain the electrochemical (i.e., HCP and ER) results from the SEM analysis, indicating the inhibition of corrosion-induced surface flaws. Therefore, the probability of ReC corrosion damage transitioning from the MiC zone to a passive state LoC area with 500-4000 ppm JAL or PAL additions in the concrete mix.

A pictorial articulation ascribes the corrosion-inhibiting mechanism of MS in CB without (control) and with 2000 ppm PAL in an ambient environment, as illustrated in Figure 13. This graphic is leveled in findings derived from a wide array of experimental methodologies, including screening tests, UV-Vis, FTIR, GC-MS, UHPLC, HCP, ER, and SEM analyses.

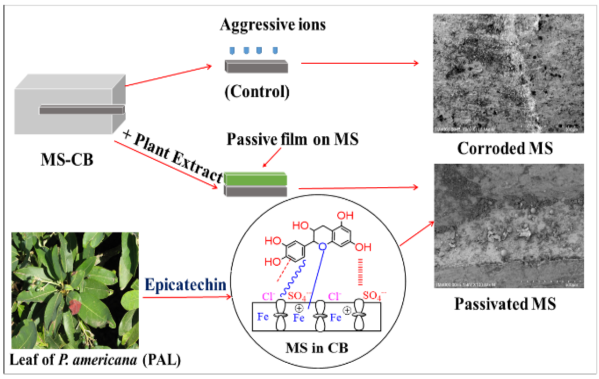

------	**Physical Adsorption (due to electrostatic interaction)**
——	**Chemical Adsorption (due to co-ordinate covalent bond)**
∿∿∿	**Chemical Adsorption (due to p-electrons interaction)**
⦀⦀⦀	**Chemical Adsorption (due to donor-acceptor interaction)**

Fig. 13. Schematic graph showing corrosion inhibiting mechanism of MS-CBs.

The corrosion-inhibiting mechanism of the MS-CBs, along with associated adsorption phenomena, results from the displacement of aggressive ions and molecules from the surface of the MS rebar. Such interactions are possible by electron transfer between the electronegative elements—oxygen, nitrogen, and sulfur in the PAL extract and the iron substrate. Such interactions, which may involve either chemical or physical adsorption or a combination thereof, contribute significantly to the enhanced protection of the MS rebar from corrosion induced by the reinforced concrete beam (Fig. 13), as illustrated the following four processes.

* Phyto-molecule (PM) protonate in concrete to form positively charged ions, which adsorb to the MS by physical adsorption or electrostatic interactions with negatively charged ions (Cl^-, SO_4^{2-}) in the concrete matrix, until they thoroughly shield the reactive anions, enhancing the corrosion-inhibition [22].
* Chemical adsorption (CA) occurs through the formation of coordination bonds between the lone-

pair electrons of O or N in PM and the vacant d-orbitals of Fe on the rebar surface [49], helping to prevent corrosion by blocking aggressive ions.

* CA promoted by π-electron interactions between an aromatic ring of PM and the vacant d-orbitals of Fe on the rebar, to assemble a passive film with high resilience to enhance the corrosion-inhibition [45].
* CA due to retro-donation or vice versa between d-electrons of Fe and empty antibonding molecular orbitals of PM constituents [43].

4 Conclusions

An anti-corrosive effect of plant-based extracts as concrete admixtures was explored with *in situ* electrochemical analysis with periodic monitoring of HCP and ER values of reinforced rebar in concrete beam (CB). Based on the findings of this study, it was concluded that the leaf extracts of *Justicia adhatoda* (JAL) and *Persea americana* (PAL) exhibit significant potential as green, eco-friendly corrosion inhibitors for steel-reinforced concrete. Phytochemical screening along with UV-visible, FTIR, and UHPLC analyses, confirmed the presence of key bioactive compounds such as phenols, alkaloids, flavonoids, tannins, and glycosides in both extracts.

Shifting of HCP and ER values of reinforced-SR from the zone of MiC or HiC (about 90% or more probability of corrosion) to LoC (Less than 10% probability of corrosion) when plant extracts are admixed to ReC. When added to concrete in concentrations ranging from 500 to 4000 ppm, these extracts notably enhanced the corrosion resistance of reinforcing steel bars, with effectiveness observed even at the lowest concentration. Surface analysis of SR in different conditions is in agreement with the prediction made by qualitative *in situ* electrochemical analysis.

These results consistently indicate that JAL and PAL are promising candidates for the development of sustainable anti-corrosive concrete additives, with the potential to extend the service life of reinforced concrete infrastructure and reduce corrosion-related deterioration. Besides, these plant-derived phyto-constituted extracts, as we believe, have diverse applications, including reinforced concrete additives, functioning as anticorrosion agents. It should not be limited only to academic research but also to industrial applications.

The authors acknowledge Dr. M.A. Fickenscher and Mr. N.K. Pandey from the University of Cincinnati, USA, for their contributions to SEM/EDS and GC-MS analysis, respectively. Additionally, they thank the University of Lucknow, India, particularly Dr. Anant Ram Rathor and Mr. Gulab Singh, for providing essential analytical facilities for UHPLC-MS.

References

1. J-Q. Wu, Z. Lu, Y-T. Chen, B. Ghiassi, W. Shi, B. Li, Mechanical properties and cracking behavior of lightweight engineered geopolymer composites with fly ash cenospheres. *Constr. Build. Mater.* **400**, 132622 (2023). https://doi.org/10.1016/j.conbuildmat.2023.132622
2. S. Ashraf, M. Rucka, Comparative study on fracture evolution in steel fiber and bar reinforced concrete beams using acoustic emission and digital image correlation techniques. *Case Stud. Constr. Mater.* **20**, e03359 (2024). https://doi.org/10.1016/j.cscm.2024.e03359
3. R. R. Hussain, Passive layer development and corrosion of steel in concrete at the nano-scale. *J. Civ. Environ. Eng.* **04**, e116 (2014). https://doi.org/10.4172/2165-784X.1000e116
4. K. N. Hoque, F. Presuel-Moreno, Long-term corrosion behavior of reinforced concrete: impact of supplementary cementitious materials and reservoir size under accelerated chloride ingress. *Const. Mater.* **5**, 33 (2025). https://doi.org/10.3390/constrmater5020033
5. A. Hameed, M. F. Afzal, A. Javed, A. M. Rasool, M. Qureshi, A. Mehrabi, I. Ashraf, Behavior and performance of reinforced concrete columns subjected to accelerated corrosion. *Metals*. **13**, 930 (2023). http://dx.doi.org/10.3390/met13050930
6. S. Akduman, H. Öztürk, Effect of reinforcement corrosion on structural behavior in reinforced concrete structures according to initiation and propagation periods. *Buildings*, **14**(12), 4026 (2024). http://dx.doi.org/10.3390/buildings14124026
7. M. S. H. S. Mohammed, R. S. Raghavan, G. M. S. Knight, V. Murugesan, Macrocell corrosion studies of coated rebars. *Arab. J. Sci. Eng.,* **39**, 3535–3543 (2014). https://doi.org/10.1007/s13369-014-1006-x
8. S. A. Civjan, J. M. Lafave, J. Trybulski, D. Lovett, J. Lima, D. W. Pfeifer, Effectiveness of corrosion inhibiting admixture combinations in structural concrete. *Cem. Concr. Compos.* **27**, 688–703 (2005). https://doi.org/10.1016/j.cemconcomp.2004.07.00
9. H. Qian, J. Mao, S. Ye, Z. Xu, S. Chen, Y. Liu, D. Yan, Coated rebars for reinforced concrete structures: A review. *J. Build. Eng.* **109**, 113000 (2025). https://doi.org/10.1016/j.jobe.2025.113000
10. R. Drochytka, M. Ledl, J. Bydzovsky, N. Zizkova, J.J. Bester, Use of secondary crystallization and fly ash in waterproofing materials to increase concrete resistance to aggressive gases and liquids. *Adv. Civ. Eng.* **2019**, 7530325 (2019). https://doi.org/10.1155/2019/7530325
11. J. Li, S. Li, M. A. Haque, B. Chen, Water-resistance performance analysis of Portland composite concrete containing waterproofing liquid membrane. *J. Build. Eng.* **76**, 106889 (2023). https://doi.org/10.1016/j.jobe.2023.106889
12. F. Wang, T. Xie, J. Ou, M. Xue, W. Li, Cement based superhydrophobic coating with excellent robustness and solar reflective ability. *J. Alloys Compd.* **823**, 153702 (2020). https://doi.org/10.1016/j.jallcom.2020.153702
13. R. Kumar, B. Bhattacharjee, Porosity, pore size distribution, and in situ strength of concrete. *Cem.*

Con. Res. **33**, 155–164 (2003). https://doi.org/10.1016/S0008-8846(02)00942-0
14. V. G. Cappellesso, N. S. Petry, D. C. C. D. Molin, A. B. Masuero, Use of crystalline waterproofing to reduce capillary porosity in concrete. *J. Build. Pathol. Rehabil.* **1**, 9 (2016). https://doi.org/10.1007/s41024-016-0012-7
15. S. C. Gnanaraj, R. B. Chokkalingam, G. L. Thankam, Effects of admixtures on the self-compacting concrete state of the art report. *IOP Conf. Ser.: Mater. Sci. Eng.* **1006**, 012038 (2020). https://doi.org/10.1088/1757-899X/1006/1/012038
16. M. R. Louis, L. Rani, V. Pushpa, K. Balakrishna, P. Ganesan, Mosquito larvicidal activity of avocado (*Persea americana* Mill.) unripe fruit peel methanolic extract against *Aedes aegypti*, *Culex quinquefasciatus* and *Anopheles stephensi*. *South Afr. J. Bot.* **133**, 1–4 (2020). http://dx.doi.org/10.1016/j.sajb.2020.06.020
17. D. J. Bhuyan, M. A. Alsherbiny, S. Perera, M. Low, A. Basu, O. A. Devi, M. S. Barooah, C. G. Li, K. Papoutsis, The odyssey of bioactive compounds in avocado (*Persea americana*) and their health benefits. *Antioxidants (Basel, Switzerland)*. **8**, 426 (2019). https://doi.org/10.3390/antiox8100426
18. A. C. Ehiemere, R. O. Anyanwu, P. Emele, U. G. Nwokeke, Anti-corrosion potentials of fresh extracts of old *Persea americana* var. *Americana* seed in 0.5 m H_2SO_4 on mild steel. *Chem. Mater. Res.* **13**, 60–71 (2021). http://dx.doi.org/10.7176/CMR/13-2-03
19. K. Muazu, M. M. Aliyu, A. T. Mohammed, S. Lasisi, R. Dahiru, I.Y. Suleiman, Ethanol extract of *Avocado* leaf as corrosion inhibitor for the protection of mild steel in acidic environment. *J. Mater. Environ. Sci.* **13**, 1343–1354 (2022). http://dx.doi.org/10.6084/m9.figshare.21699587
20. Isha, P. Kumar, A. N. Singh, An overview of *Justicia adhatoda*: A medicinal plant but native invader in India. *Conservation*. **5**, 2 (2025). https://doi.org/10.3390/conservation5010002
21. K. S. Beenakumari, *Justicia adhatoda* (Vasaka) leaf extracts as eco-friendly corrosion inhibitor for mild steel in potable water. *Orient. J. Chem.* **29**, 369–373 (2013). http://dx.doi.org/10.13005/ojc/290159
22. ASTM C1582/C1582M-11, *Standard Specification for Admixtures to Inhibit Chloride Induced Corrosion of Reinforcing Steel in Concrete.* In Annual book of ASTM standards, ASTM International, West Conshohocken, USA (2017) 10 https://doi.org/10.1520/C1582_C1582M-11R17E01
23. M. Gautam, N. P. Bhattarai, J. Bhattarai, Leaf-based extracts of Nepal origin plants as efficient inhibitors for controlling rebar corrosion in concrete pore solution. *Int. J. Corros. Scale Inhib.* **13**, 2087–2111 (2024). http://dx.doi.org/10.17675/2305-6894-2024-13-4-10
24. ASTM C876-22b, *Standard Test Method for Corrosion Potentials of Uncoated Reinforcing Steel in Concrete.* In: Annual book of ASTM standards, ASTM International, West Conshohocken, USA (2022). https://doi.org/10.1520/C0876-22B
25. A. Basit, T. Shutian, A. Khan, S. M. Khan, R. Shahzad, A. Khan, M. Khan, Anti-inflammatory and analgesic potential of leaf extract of *Justicia adhatoda* L. (Acanthaceae) in carrageenan and formalin-induced models by targeting oxidative stress. *Biomed. Pharmacother.* **153**, 113322 (2022). https://doi.org/10.1016/j.biopha.2022.113322
26. A. Thoume, I. N. Irahal, N. Benzbiria, D. B. Left, R. Achagar, A. Elmakssoudi, A. El foulani, M. Dakir, M. Azzi, N. Bourhim, M. Zertoubi, In vitro and in silico antibacterial and anti-corrosive properties of Persea americana leaves extract as an environmentally friendly corrosion inhibitor for carbon steel in a hydrochloric acid medium. *Colloids Surf. A: Physicochem. Eng. Aspects.* **674**, 131848 (2023). https://doi.org/10.1016/j.colsurfa.2023.131848
27. R. Paji, A. Samrot, B. R. Fernando, P. Kumar, R. Geetika, V. Sharma, K. Dhanabal, Extraction, characterization and *in vitro* bioactivity evaluation of alkaloids, flavonoids, saponins and tannins of *Cassia alata, Thespepia populnea, Euphorbia hirta* and *Wrightia tinctoria*. *Rasayan J. Chem.* **12**, 123–137 (2019). http://dx.doi.org/10.31788/RJC.2019.1214054
28. L. Akinpelu, O. Idowu, G. Ogundepo, A. Adegoke, G. Olayiwola, T. Idowu, Spectroscopic analysis and anti-inflammatory effects of *Milicia excelsa* (Moraceae) leaf and fractions. *GSC Biol. Pharm. Sci.* **6**, 51–60 (2019). http://dx.doi.org/10.30574/gscbps.2019.6.3.0035
29. A. Williams, D. Flemming, *Spectroscopic Methods in Organic Chemistry*, (Springer, 2019) 55–81. https://doi.org/10.1007/978-3-030-18252-6
30. P. Somchaidee, K. Tedsree, Green synthesis of high dispersion and narrow size distribution of zero-valent iron nanoparticles using guava leaf (*Psidium guajava* L) extract. *Adv. Nat. Sci.: Nanosci. Nanotechnol.* **9**, 035006 (2018). https://doi.org/10.1088/2043-6254/aad5d7
31. A. Barbasz, M. Oćwieja, J. Barbasz, Cytotoxic activity of highly purified silver nanoparticles sol against cells of human immune system. *Appl. Biochem. Biotechnol.* **176**, 817-834 (2015). https://doi.org/10.1007/s12010-015-1613-3
32. C. Yuan, Y. Li, Q. Li, R. Jin, L. Ren, Purification of tea saponins and evaluation of its effect on alcohol dehydrogenase activity. *Open Life Sci.* **13**, 56–63 (2018). https://doi.org/10.1515/biol-2018-0008
33. D. I. Njoku, M. A. Chidiebere, K. L. Oguzie, C. E. Ogukwe, E.E. Oguzie, Corrosion inhibition of mild steel in hydrochloric acid solution by the leaf extract of *Nicotiana tabacum*. *Adv. Mater. Corros.* **1**, 54–61 (2013). https://api.semanticscholar.org/CorpusID:92074940
34. J. Coates, Interpretation of infrared spectra, a practical approach, in R. A. Meyers (Ed.),

Encyclopedia of Analytical Chemistry (1st ed.), Wiley (2000).
35. A. Sulistiawan, W. Setyaningsih, A. Rohman, A new FTIR method combined with multivariate data analysis for determining aflatoxins in peanuts (*Arachis hypogaea*). *J. Appl. Pharm. Sci.* **12**, 199–206 (2022). https://doi.org/10.7324/JAPS.2022.120720
36. P. P. Yue, Y. J. Hu, G. Q. Fu, C. X. Sun, M. F. Li, F. Peng, R. C. Sun, Structural differences between the lignin-carbohydrate complexes (LCCs) from 2- and 24-months old bamboo (*Neosinocalamus affinis*). *Int. J. Mol. Sci.* **19**, 1 (2018). https://doi.org/10.3390/ijms19010001
37. J. M. Barcelo, A. M. Gatchallan, I. J. B. Aquino, D. R. E. Ollero, F. L. D. Cortez, T. M. Costales, L. A. Q. Marzo, FTIR spectrum and anti-mutagenicity of *Coffea arabica* pulp and *Arachis hypogaea* test in relation to their *in vitro* antioxidant properties. *Asia Pac. J. Multidiscip. Res*. **3**, 99–108 (2015)
38. M. Maczka, A. Ciupa, A. Gągor, A. Sieradzki, A. Pikul, B. Macalik, M. Drozd, Perovskite metal formate framework of [NH_2-CH^+-NH_2] Mn ($(HCOO)_3$]: phase transition, magnetic, dielectric, and phonon properties. *Inorg. Chem.* **53**, 5260–5268 (2014). https://doi.org/10.1021/ic500479e
39. K. K. Veedu, T. P. Kalarikkal, N. Jayakumar, N. K. Gopalan, Anticorrosive performance of *Mangifera indica* L. leaf extract-based hybrid coating on steel. *ACS Omega*. **4**, 10176–10184 (2019)
40. V. M. Oliveira, R. C. A. Neri, F. T. D. Monte, N. A. Roberto, H. M. S. Costa, C. R. D. Assis, A. L. F. Porto, Crosslink-free collagen from *Cichla ocellaris*: structural characterization by FTIR spectroscopy and densitometric evaluation. *J. Mole. Struct.* **1176**, 751–758 (2019). https://doi.org/10.1016/j.molstruc.2018.09.023
41. B. Kumar, L. Cumbal, UV-Vis, FTIR and antioxidant study of *Persea americana* (avocado) leaf and fruit: a comparison. *Rev. Fac. Cien. Quím.* **14**, 13–20 (2016)
42. M. Bedair, L.W. Sumner, Current and emerging mass-spectrometry technologies for metabolomics. *Trends Anal. Chem.* **27**, 238–250 (2008). https://doi.org/10.1016/j.trac.2008.01.006
43. G. Jayapriya, F. Gricilda Shoba, GC-MS analysis of bioactive compounds in methanolic leaf extracts of Justicia adhatoda (Linn.). *J. Pharmacog. Phytochem.* **4**, 113–117 (2015)
44. I. M. Abu-Reidah, M. S. Ali-Shtayeh, R. M. Jamous, D. Arráez-Román, A. Segura-Carretero, Comprehensive metabolite profiling of *Arum palaestinum* (Araceae) leaves by using liquid chromatography–tandem mass spectrometry. *Food Res. Int.* **70**, 74–86 (2015). http://dx.doi.org/10.1016/j.foodres.2015.01.023
45. M. Gautam, D. B. Subedi, J. R. Dhungana, M. Dhakal, K. P. Bohara, N. P. Bhattarai, J. Bhattarai, A sustainable approach for mitigating rebar corrosion in adverse conditions using *Phyllanthus emblica* (L.) leaf extract as concrete scale inhibitor. *Int. J. Corros. Scale Inhib.* **14**, 1522–1554 (2025). https://doi.org/10.17675/2305-6894-2025-14-3-26
46. M. Gautam, N. P. Bhattarai, J. Bhattarai, *Sisamum indicum* leaf extract as environmentally benign inhibitor to mitigate mild steel corrosion in cement pore solution. *J. Inst. Sci. Technol.* **30**, 101–113 (2025). https://doi.org/10.3126/jist.v30i1.74723
47. M. H. Rahmani, A. Dehghani, M. Salamati, G. Bahlakeh, B. Ramezanzadeh, Mango extract behavior as a potent corrosion inhibitor against simulated chloride-contaminated concrete pore solution; coupled experimental and computer modeling studies. *J. Indus. Eng. Chem.* **130**, 368–381 (2024). https://doi.org/10.1016/j.jiec.2023.09.040
48. L. Casanova, F. Ceriani, E. Messinese, L. Paterlini, S. Beretta, F.M. Bolzoni, M. Pedeferri, Recent advances in the use of green corrosion inhibitors to prevent chloride-induced corrosion in reinforced concrete. *Materials* (Basel, Switzerland). **16**, 7462 (2023). https://doi.org/10.3390/ma16237462
49. C. Verma, A. R. Pathania, I. Barsoum, K. Y. Rhee, Y. Qiang, A. Alfantazi, Coordination chemistry in corrosion science and engineering: Role of coordination bonding and coordination materials. *Coord. Chem. Rev.* **549**, 217258 (2026). https://doi.org/10.1016/j.ccr.2025.217258